



Published in final edited form as:

*J Comp Neurol.* 2017 October 15; 525(15): 3177–3189. doi:10.1002/cne.24257.

## Phenotyping of nNOS neurons in the postnatal and adult female mouse hypothalamus

Konstantina Chachlaki<sup>1,2</sup>, Samuel A. Malone<sup>1,2</sup>, Emily Qualls-Creekmore<sup>3</sup>, Erik Hrabovszky<sup>4</sup>, Heike Münzberg<sup>3</sup>, Paolo Giacobini<sup>1,2</sup>, Fabrice Ango<sup>5,6</sup>, and Vincent Prevot<sup>1,2</sup>

<sup>1</sup>Inserm, Laboratory of Development and Plasticity of the Neuroendocrine Brain, Jean-Pierre Aubert Research Center, U1172, Lille, France

<sup>2</sup>University of Lille, FHU 1000 days for Health, School of Medicine, Lille, France

<sup>3</sup>Departments of Central Leptin Signaling, Pennington Biomedical Research Center, Louisiana State University System, Baton Rouge, Louisiana

<sup>4</sup>Institute of Experimental Medicine, Laboratory of Endocrine Neurobiology, Budapest, Hungary

<sup>5</sup>Inserm, Laboratory of Development of GABAergic circuit, IGF, U1191, Montpellier, France

<sup>6</sup>University of Montpellier, CNRS UMR5203, Montpellier, France

### Abstract

Neurons expressing nitric oxide (NO) synthase (nNOS) and thus capable of synthesizing NO play major roles in many aspects of brain function. While the heterogeneity of nNOS-expressing neurons has been studied in various brain regions, their phenotype in the hypothalamus remains largely unknown. Here we examined the distribution of cells expressing nNOS in the postnatal and adult female mouse hypothalamus using immunohistochemistry. In both adults and neonates, nNOS was largely restricted to regions of the hypothalamus involved in the control of bodily functions, such as energy balance and reproduction. Labeled cells were found in the paraventricular, ventromedial, and dorsomedial nuclei as well as in the lateral area of the hypothalamus. Intriguingly, nNOS was seen only after the second week of life in the arcuate nucleus of the hypothalamus (ARH). The most dense and heavily labeled population of cells was found in the organum vasculosum laminae terminalis (OV) and the median preoptic nucleus (MEPO), where most of the somata of the neuroendocrine neurons releasing GnRH and controlling reproduction are located. A great proportion of nNOS-immunoreactive neurons in the OV/MEPO and ARH were seen to express estrogen receptor (ER)  $\alpha$ . Notably, almost all ER $\alpha$ -immunoreactive cells of the OV/MEPO also expressed nNOS. Moreover, the use of EYFP<sup>Vglut2</sup>, EYFP<sup>Vgat</sup>, and GFP<sup>Gad67</sup> transgenic mouse lines revealed that, like GnRH neurons, most hypothalamic nNOS neurons have a glutamatergic phenotype, except for nNOS neurons of the ARH, which are GABAergic. Altogether, these observations are consistent with the proposed role of nNOS neurons in physiological processes.

## Keywords

Nitric oxide; estrogen receptor; development; GABA; glutamate; GnRH neurons; hypothalamus; immunofluorescence; RRID:IMSR\_JAX:007677; RRID:IMSR\_JAX:016963; RRID:IMSR\_JAX:016962; RRID:IMSR\_JAX:006148; RRID:AB\_310305; RRID:AB\_300798; RRID:AB\_2534017; RRID:AB\_2535865; RRID:AB\_2340375; RRID:AB\_2651133; RRID:SCR\_014199

## 1 | INTRODUCTION

Nitric oxide (NO) is a chemical transmitter with an extremely diverse role in the mammalian central and peripheral nervous systems (Garthwaite, 2008; Garthwaite, 2016; Steinert, Chernova, & Forsythe, 2010). Therefore, it comes as no surprise that neurons expressing neuronal NO synthase (nNOS) are represented by a variety of subpopulations of cells that differ in terms of their genetic specification and molecular characterization, with their only common property being their ability to synthesize NO. This heterogeneity in the origins of nNOS cells as well as the nature of the neurotransmitters they may co-express has been studied in several regions of the brain, such as the hippocampus, the neocortex, the nucleus of the solitary tract, and the olfactory bulb (Crespo et al., 2003; Fujimoto, Konno, Watanabe, & Jinno, 2016; Giuli, Luzzi, Poyard, & Guellaen, 1994; Lin, 2009; Tricoire & Vitalis, 2012; von Bartheld & Schober, 1997). However, our knowledge concerning the development and molecular identity of the cell populations expressing nNOS in the hypothalamus is extremely limited.

Results obtained from genetically modified mouse models harboring either mutations in the *Nos1* gene (Gyurko, Leupen, & Huang, 2002; Huang, Dawson, Bredt, Snyder, & Fishman, 1993) or the selective inactivation of specific genes in nNOS-expressing cells (Leshan, Greenwald-Yarnell, Patterson, Gonzalez, & Myers, 2012) suggest that hypothalamic nNOS neurons play vital roles in the control of reproduction (Gyurko et al., 2002; Hanchate et al., 2012; Messina et al., 2016) and energy homeostasis (Leshan et al., 2012; Sutton et al., 2014), as well as in the crosstalk between these two vital functions (Bellefontaine et al., 2014). This crosstalk is also thought to involve, at least in part, GABAergic neurons (Martin et al., 2014; Zuure, Roberts, Quennell, & Anderson, 2013). Except for partial information from recent studies (Marshall, Desrozier, McLennan, & Campbell, 2016), the issue of whether GABA and NO are co-synthesized in discrete populations of hypothalamic neurons remains unexplored.

The regulation of reproduction mediated by hypothalamic nNOS neurons is principally thought to occur in the preoptic region at the median preoptic nucleus (MEPO) and the organum vasculosum laminae terminalis (OV), where neurons expressing nNOS and gonadotropin-releasing hormone (GnRH) are co-distributed (d'Anglemont de Tassigny et al., 2007; Hanchate et al., 2012; Herbison, Simonian, Norris, & Emson, 1996) and interact functionally (Bellefontaine et al., 2014; Cla-sadonte, Poulain, Beauvillain, & Prevot, 2008). The activity of nNOS in the preoptic region has been shown to be tightly regulated by circulating estrogen levels (d'Anglemont de Tassigny et al., 2007; Parkash et al., 2010) and to be required for estrous cyclicity (d'Anglemont de Tassigny et al., 2007). In particular, nNOS activity has been shown to restrain the activity of the hypothalamo-pituitary-gonadal

(HPG) axis during phases of the estrous cycle at which circulating levels of estrogens are low, and to be required for the onset of the LH surge induced by gonadal steroids in mice (Hanchate et al., 2012). Results from recent studies knocking out estrogen receptor alpha (ER $\alpha$ ) expression selectively in glutamatergic neurons have shown, unexpectedly, that glutamatergic neurons, which tightly regulate nNOS activity (Garthwaite, Charles, & Chess-Williams, 1988) and have long been known to be potent activators of the HPG axis (Brann & Mahesh, 1991; Claypool, Kasuya, Saitoh, Marzban, & Terasawa, 2000; Urbanski & Ojeda, 1990), not only play a role in the estrogen-mediated positive-feedback phase, which triggers the preovulatory GnRH surge, but also in the negative feedback loop (Cheong, Czielesky, Porteous, & Herbison, 2015). These findings raise the hitherto unexplored possibility that discrete populations of glutamatergic neurons co-express nNOS in the hypothalamus.

In addition to its regulatory role in the adult, nNOS is also expressed in the hypothalamus during early life (Edelmann, Wolfe, Scordalakes, Rissman, & Tobet, 2007), suggesting a role for NO in the maturation of GnRH neurons during postnatal development via the regulation of GnRH mRNA expression (Messina et al., 2016), a phenomenon that could be critical for sexual maturation (Prevot, 2015).

In the present study, we systematically analyzed the distribution of nNOS in the female mouse hypothalamus during postnatal development and in adulthood. In addition, to determine when nNOS neurons become competent in sensing the estrogenic signal, we studied the distribution of cells expressing ER $\alpha$  in both the developing and adult mouse hypothalamus. Furthermore, we used *EYFP<sup>Vslut2</sup>*, *EYFP<sup>Vsat</sup>* and *GFP<sup>Gad67</sup>* transgenic mice to further characterize the neurochemical phenotype of nNOS neurons in the hypothalamus.

## 2 | MATERIALS AND METHODS

### 2.1 | Animals and tissue preparation

Animal studies were approved by the Institutional Ethics Committees for the Care and Use of Experimental Animals of the Universities of Lille, Montpellier and Louisiana; all experiments were performed in accordance with the guidelines for animal use specified by the European Union Council Directive of September 22, 2010 (2010/63/EU). All mice were group-housed in a temperature-controlled room (21–22°C) with a 12 hr light/dark cycle and ad libitum access to food and water. Experiments were undertaken at different stages of postnatal development: at postnatal days 11 (P11) and 23 (P23), which are key phases of sexual maturation that have particularly been well characterized in females (see Discussion), and adulthood. C57Bl/6J *Gad67::Gfp* (GFP<sup>Gad67</sup>, line G42; RRID:IMSR\_JAX:007677) mice, in which GFP is expressed in parvalbumin-positive cells, were engineered as detailed elsewhere (Ango et al., 2004). C57Bl/6J *Vglut2::Cre* (RRID:IMSR\_JAX:016963). and *Vgat::Cre* (RRID:IMSR\_JAX:016962) mice were generously provided by Dr. Bradford B. Lowell, Beth Israel Deaconess Medical Center and Harvard Medical School (Vong et al., 2011) and crossed with EYFP<sup>loxP-Stop-loxP</sup> mice (RRID:IMSR\_JAX:006148) to generate EYFP<sup>Vglut2</sup> and EYFP<sup>Vgat</sup> mice. P11 (infantile period,  $n = 4$ ), P23 (juvenile period,  $n = 4$ ) and diestrous adult (P60–P80,  $n = 8$ ) female mice were deeply anesthetized with pentobarbital (50–90 mg/kg i.p.) and perfused transcardially with 0.9% saline, followed by ice-cold 4% paraformaldehyde in 0.1M sodium phosphate buffer (PB), pH 7.4. The brains

were quickly removed, post-fixed in the same fixative containing 20% sucrose for 4 hr (postnatal) or overnight (adult) at 4°C, and immersed in 20% sucrose in 0.02M potassium phosphate buffered saline (KPBS) at 4°C overnight. The brains were embedded in OCT medium (Tissue-Tek®, Sakura, Villeneuve d'Ascq, France), frozen in isopentane (−55°C) and stored at −80°C until sectioning. Using a cryostat, serial frozen sections (16 and 30 µm thick for P11-P23 and adult brains, respectively) were cut and collected on chrome-alum-gelatin-coated slides.

## 2.2 | Antibody characterization

All primary antibodies used are listed in Table 1, and the labeling observed corresponded to the cellular morphology and distribution patterns demonstrated in previous publications.

## 2.3 | Immunohistochemistry

Sections were washed three times in PB 0.1M for 5 min each and then microwaved in 10 mM citrate buffer pH 6.0 (4 min at 800 W followed by 2 × 5 min at 400 W) for antigen unmasking. Sections were then washed in PB 0.1M, and incubated in blocking solution (5% donkey serum + 0.3% Triton X-100) in PB 0.1M for 60 min. Then, sections were incubated in rabbit anti-ER $\alpha$  (1/500; Millipore, Cat# 06–935 Lot#2708536, RRID:AB\_310305) or guinea pig anti-GnRH (1/3000 raised by Dr. Erik Hrabovszky, Laboratory of Endocrine Neurobiology, Institute of Experimental Medicine of the Hungarian Academy of Sciences, Budapest, Hungary) and sheep anti-nNOS (1/10,000; generous gift from Dr. P. C. Emson, Medical Research Council, Laboratory for Molecular Biology, Cambridge, UK) and, when required, chicken anti-GFP antibody (1/500; Abcam, Cat# ab13970 Lot#GR236651–14 RRID:AB\_300798) in blocking solution for 48 hr at 4°C. After incubation in the primary antibody, sections were rinsed with PB 0.1M three times for 10 min each and then incubated in the secondary antibody: Alexa-568-conjugated donkey anti-rabbit or anti-guinea pig (Thermo Fisher Scientific Cat# A10042, RRID:AB\_2534017), Alexa-647-conjugated donkey anti-sheep (Thermo Fisher Scientific Cat# A-21448, RRID:AB\_2535865) and donkey anti-chicken Alexa 488 (Jackson ImmunoResearch Labs Cat# 703–545-155, RRID:AB\_2340375) for 60 min at room temperature. Sections were then washed, counterstained with Hoechst (1/10,000; Thermo Fisher Scientific Cat# H3569, RRID:AB\_2651133) for 5 min, washed twice for 5 min and coverslipped with Mowiol coverslip mounting solution.

## 2.4 | Image acquisition

Images were acquired with a Zeiss Axio Imager Z2 microscope (Zeiss, Germany). Alexa 488 was imaged using a 495 nm beam splitter with an excitation wavelength set at 450/490 nm and an emission wavelength set at 500/550 nm. Alexa 568 was imaged using a 570 nm beam splitter with an excitation wavelength set at 538/562 nm and an emission wavelength set at 570/640 nm. Alexa 647 was imaged by using a 660 nm beam splitter with an excitation wavelength set at 625/ 655 nm and an emission wavelength set at 665/715 nm. Nuclear staining (Hoechst) was imaged by using a 395 nm beam splitter with an excitation wavelength set at 335/383 nm and an emission wavelength set at 420/470 nm. Images were acquired with a Plan-Apochromat 20X objective (numerical aperture NA = 0.80; thread type M27). Z-stack images were taken every 0.49 µm, for a total of 28.90 µm for adult sections,

and 6.86  $\mu\text{m}$  for P11 and P23 sections. High magnification photomicrographs represent maximal intensity projections derived from 20 to 25 triple-ApoTome images collected using the Z-stack module of the AxioVision 4.6 system and a Zeiss 63X oil-immersion objective (NA 1.4). Images to be used for figures were adjusted for brightness and contrast using Photoshop (Adobe Systems, San Jose, CA, RRID:SCR\_014199).

## 2.5 | Cell counts and analysis

The nomenclature of brain regions used in this article corresponds to that described in the mouse Allen brain atlas ([http://mouse.brainmap.org/experiment/thumbnails/100048576?image\\_type=atlas](http://mouse.brainmap.org/experiment/thumbnails/100048576?image_type=atlas)) (Lein et al., 2007). The quantification of nNOS neurons co-expressing ER $\alpha$  or GFP<sup>Gad67</sup> expression was undertaken by counting the number of single-labeled or double-labeled cells in the OV and MEPO, represented by plate 49 of the Allen Developing Mouse Brain Atlas, and in the arcuate (ARH), ventromedial (VMH) and dorsomedial (DMH) nuclei of the hypothalamus, represented by plate 70. Cell counts were carried out unilaterally in the OV/MEPO, ARH, VMH, and DMH, delimited by Hoechst nuclear staining, over a total surface area of 676  $\mu\text{m}$  X 676  $\mu\text{m}$  for the OV/MEPO and 1.28 mm X 1.87 mm for the ARH, VMH, and DMH. Single-plane images were acquired from four 16- $\mu\text{m}$ -thick frontal sections separated by 32  $\mu\text{m}$  in P11 and P23 mice, and two 30- $\mu\text{m}$ -thick frontal sections separated by 30  $\mu\text{m}$  in adult mice, by using the ApoTome technology. Cells expressing nNOS and/or ER $\alpha$  immuno-reactivity were counted in each structure delineated by the Hoechst staining. To ensure that each cell was only counted once, only cells for which the Hoechst-labeled nucleus could be visualized were taken into consideration. The results from our analysis of four or two sections per P11/P23 and adult animals, respectively, were combined and values from each mouse were averaged to determine mean counts and SEM for each age group. All data were analyzed using the nonparametric multiple-comparison Kruskal-Wallis test. Statistical significance was accepted if  $P$  was  $<0.05$ .

## 3 | RESULTS

The immunoreactive signal for nNOS in the CNS is highly abundant in the hypothalamus of female mice (Table 2), with a particularly dense distribution in the OV and the MEPO (Figure 1a). As indicated in Table 2 and below in the text, nNOS immunoreactivity was assessed as being of the “highest density”, “high density”, “moderate density”, “low density”, and “undetectable” based on both signal strength and the number of labeled cells. This labeling appeared to be specific because no cellular immunoreactive signal was observed when the same antibody was used on sections obtained from nNOS-null mice (data not shown).

### 3.1 | Expression of nNOS immunoreactivity in adults

In the preoptic area of adult female mice, besides the dense expression of nNOS in the OV/MEPO (Figure 1a), moderate levels of nNOS labeling were also found in the anteroventral periventricular nucleus (AVPV) (Figure 1b) and the medial preoptic area (MPO) (Figure 1b). An nNOS immunoreactive signal was clearly seen in cell bodies of the supraoptic nucleus (SO) (Figure 1c), the paraventricular hypothalamic nucleus (PVH) (Figure 1d) and the lateral hypothalamic area (LHA) (Figure 1c), but appeared to be absent from the

suprachiasmatic hypothalamic nucleus (SCH) (Figure 1c). In the tuberal region of the hypothalamus, nNOS immunoreactivity was also found in neuronal cell bodies of the dorsomedial hypothalamic nucleus (DMH) (Figure 1e), the ventrolateral part of the ventromedial hypothalamic nucleus (VMHvl) (Figure 1e), the arcuate nucleus of the hypothalamus (ARH) (Figure 1e), the LHA, and the ventral premammillary nucleus (PMv) (Figure 1f), whereas only rare nNOS-immunoreactive cell bodies were seen in the posterior periventricular nucleus (PVp) (Figure 1f).

### 3.2 | Expression of nNOS-immunoreactivity in postnatal brains

As shown in Table 2 and Figure 2, the pattern of nNOS protein expression in the hypothalamus of P11 and P23 animals resembled that of adult mice, with two marked exceptions being the SCH and the ARH. nNOS immunoreactivity did not appear to vary across postnatal development (Table 2) in the OV/MEPO (Figures 2a,b and 1a), AVPV (Figures 2c,d and 1b), PVH (Figure 2g,h), MPO (Figures 2c,d and 1b), and LHA (Figures 2e,f and 1c). In contrast, nNOS immunoreactivity was seen to decrease drastically in the SCH between P11 and adulthood (p11:  $22.6 \pm 0.88$ , p23:  $13.67 \pm 0.88$  and adult:  $4.66 \pm 2.73$ ,  $n = 3$  per group) (Figure 2e,f). In the tuberal region of the hypothalamus, nNOS expression was consistent between adult and postnatal brains in most nuclei, such as the VMH, DMH, PVp, and PMv (Table 2) (Figure 2i-l). However, striking differences in nNOS expression depending on age did exist in the ARH. While nNOS-immunoreactive neurons could be easily seen in the ARH of P23 ( $22.25 \pm 0.78$ ,  $n = 3$ ) and adult female brains ( $36.5 \pm 2.76$ ,  $n = 3$ ) (Figures 1e and 2j), the nNOS signal was totally absent in the ARH at P11 ( $n = 3$ ) (Figure 2i, Table 2).

### 3.3 | Subsets of nNOS neurons express ER $\alpha$ -immunoreactivity in the hypothalamus

To determine whether hypothalamic nNOS neurons can sense estrogens during postnatal development, we studied the pattern of ER $\alpha$  immunoreactivity. ER $\alpha$  immunoreactivity was clearly detected in the majority of nNOS-positive neurons in both the OV (P11:  $74.65\% \pm 12.15$ , P23:  $67.84\% \pm 2.77$ , adult:  $82.71\% \pm 3.01$ ,  $n = 3-4$  per group) and the MEPO (P11:  $56.74\% \pm 10.47$ , P23:  $53.65\% \pm 3.46$ , adult:  $50.15\% \pm 5.97$ ,  $n = 3-4$  per group), with no significant difference in the percentage of double-labeled cells between ages (Figures 3a and 4a). Interestingly, the vast majority of the ER $\alpha$ -expressing neurons of the OV (P11:  $95.83\% \pm 1.01$ , P23:  $85.14\% \pm 5.35$ , adult:  $82.21\% \pm 7.40$ ,  $n = 3-4$  per group) and MEPO (P11:  $67.66\% \pm 6.89$ , P23:  $82.04\% \pm 7.36$ , adult:  $87.59\% \pm 4.17$ ,  $n = 3-4$  per group) corresponded to the population of nNOS-expressing neurons, leaving only a few single-labeled ER $\alpha$ -expressing neurons that did not express the nNOS protein (Figures 3a and 4a). In the AVPV, a hypothalamic structure known to play a key role in mediating the positive feedback of estradiol on the HPG axis (Herbison, 2016), nNOS neurons, which were much less abundant than in the OV/MEPO, were also seen to express ER $\alpha$  at the different ages analyzed (Figures 3b and 4b). In the ARH, another key hypothalamic structure involved in the feedback loop of gonadal estrogens (Herbison, 2016; Oakley, Clifton, & Steiner, 2009; Pinilla, Aguilar, Dieguez, Millar, & Tena-Sempere, 2012), ER $\alpha$ -immunoreactivity was detected as early as P11, as previously reported by others (Brock, De Mees, & Bakker, 2015), when nNOS immunoreactivity is not yet detectable. At P23, more than 70% of the nNOS-immunoreactive neurons of the ARH already co-expressed ER $\alpha$  ( $72.65\% \pm 5.60$ ,  $n =$



4), a proportion that persisted into adulthood ( $72.29\% \pm 7.29$ ,  $n = 3$ ) (Figures 3c and 4d). In the adult VMH, nNOS-immunoreactive cells located in the ventrolateral part of the nucleus were also seen to extensively colocalize with ER $\alpha$  ( $70.65\% \pm 6.8$ ,  $n = 3$ ) (Figure 4e), in agreement with previous reports (Okamura, Yokosuka, & Hayashi, 1994). An age-dependent increase in the proportion of nNOS cells double-labeled for ER $\alpha$  was detected in the VMH (P11:  $32.22 \pm 1.92\%$ , P23:  $47.11 \pm 1.62\%$ ,  $n = 3$ –4 per group, Kruskal-Wallis test,  $P = 0.018$ ; Dunn's multiple-comparison test, P11 vs. adult:  $P < 0.05$ ) (Figure 3c). In the DMH, ER $\alpha$ -containing cells were scattered and weakly labeled, as opposed to the large population of nNOS expressing neurons residing in this nucleus; only occasional colocalization between nNOS and ER $\alpha$  immunoreactivities was detected at any stage of postnatal development (Figures 3c and 4c). In the PMv, where there is an abundant population of nNOS neurons, only sporadic ER $\alpha$  immunoreactivity was detected, although some double-labeled cells could be found (Figures 3d and 4f).

### 3.4 | Differential expression of *Vglut2* and *Vgat* promoters in hypothalamic nNOS neurons

Immunolabeling for nNOS in the hypothalamus of adult female EYFP<sup>*Vgat*</sup> and EYFP<sup>*Vglut2*</sup> mice (which express the enhanced yellow fluorescent protein, EYFP, in cells expressing the promoters for the vesicular glutamate transporter 2 gene, *Vglut2*, and the vesicular GABA transporter gene, *Vgat*) revealed a strong segregation of the phenotype of nNOS-expressing neuronal populations depending on their anatomical localization. In the OV/MEPO as well as in the DMH and VMH, more than 85% of nNOS-immunoreactive neurons were seen to have *Vglut2* promoter activity (OV:  $85.90 \pm 2.58\%$ , MEPO:  $85.28 \pm 1.22\%$ , DMH:  $83.86 \pm 2.13\%$ , VMH:  $89.31 \pm 5.01\%$ ,  $n = 3$ ) (Figure 5a-e), while less than 15% showed *Vgat* promoter expression (OV:  $1.56 \pm 1.15\%$ , MEPO:  $1.35 \pm 0.76\%$ , DMH:  $11.45 \pm 1.74\%$ , VMH:  $2.19 \pm 0.36\%$ ,  $n = 3$ ) (Figure 5f-i), pointing to the glutamatergic identity of the vast majority of nNOS neurons in these nuclei. In contrast, *Vglut2* promoter activity was completely absent in the nNOS neurons of the ARH (Figure 5e), where virtually all nNOS-immunoreactive cells were seen to exhibit *Vgat* promoter activity, pointing to their GABAergic phenotype ( $90.93 \pm 3.91\%$ ,  $n = 3$ ) (Figure 5j).

### 3.5 | Distinct populations of nNOS neurons morphologically interact with hypothalamic GnRH neuronal cell bodies and nerve terminals

Cellular analyses of double-labeled material showed that most nNOS neurons morphologically associated with GnRH cell bodies or dendrites in the OV/MEPO expressed *Vglut2* promoter activity (Figure 6a-g). Interestingly, analysis of EYFP labeling showed that *Vglut2* promoter activity was also expressed in the majority (but not all) of the GnRH immunoreactive cells of the OV/MEPO (Figure 6a-g). These results are in agreement with previous studies attributing a glutamatergic identity to GnRH neurons (Hrabovszky, Turi, Kallo, & Liposits, 2004).

The use of the *Gad67::Gfp* G42 animal model, in which green fluorescent protein (GFP) is specifically expressed in parvalbumin-immunoreactive GABA neurons (GFP<sup>*Gad67*</sup>) (Ango et al., 2004; Chatto-padhyaya et al., 2004), allowed us to explore the specific relationship between this subpopulation of GABAergic neurons and nNOS- and GnRH-expressing cells in the hypothalamus. Although a large population of GFP<sup>*Gad67*</sup> neurons was seen to reside in

the medial septal nucleus (MS) (data not shown), an extra-hypothalamic structure known to receive reciprocal connections from the hypothalamus (Risold & Swanson, 1997; Swanson & Cowan, 1979), relatively few GFP<sup>God67</sup> neurons from the G42 mouse line were detected in the hypothalamus. While GFP<sup>God67</sup> fibers were abundantly distributed in the OV/MEPO, GFP-positive neuronal somata were only rarely seen in the preoptic region. GFP<sup>God67</sup> neurons in the OV/MEPO were never seen to co-express the nNOS protein (Figure 6h,i). Remarkably, however, several of the GFP<sup>God67</sup> neuronal somata were found to be immunoreactive for GnRH (Figure 6i-n), raising the possibility that at least a portion of the non-glutamatergic GnRH neurons that were identified in EYFP<sup>Vglut2</sup> mice could be parvalbumin-expressing GABAergic neurons. In contrast, in the ARH, 30% of the GFP<sup>God67</sup> neurons were seen to express nNOS-immunoreactivity in adult mice. Projections from GnRH neurons were observed approaching some of these nNOS-immunoreactive GFP<sup>God67</sup> neurons (inset Figure 6i-t). While EYFP<sup>Vgot</sup> signal was detectable in nearly all nNOS neurons of the ARH, only less than 5% expressed *Gad67* promoter activity (Figure 6o,p,r), indicating that the majority of nNOS neurons in the ARH belong to a different class of GABAergic cells.

## 4 | DISCUSSION

In the present study, we used immunohistochemistry to systematically examine the distribution of nNOS in the preoptic and tuberal regions of the hypothalamus in female mice. In addition, several sites in which nNOS expression changes during postnatal life were identified. Finally, according to their distinct neurochemical repertoires, three main populations of hypothalamic nNOS neurons were identified. Our findings are consistent with the proposed role of nNOS in regulating the neuroendocrine control of reproduction, and suggest that hypothalamic NO could also be involved in regulating body weight homeostasis.

It is well established that gonadal estrogens act via the brain to control the secretion of gonadotropins (follicle stimulating hormone, FSH, and luteinizing hormone, LH) by the pituitary gland and thus control gonadal growth, folliculogenesis and ovulation in females. The onset of this feedback mechanism occurs after mini-puberty, which consists of an FSH surge occurring at P12 that triggers the growth of the first pool of ovarian follicles that will ovulate at puberty (Prevot, 2015), concomitant with the decrease in circulating levels of the estrogen-binding  $\alpha$ -fetoprotein between P12 and P16 (Bakker et al., 2006; Germain, Campbell, & Anderson, 1978). The present study demonstrates that most nNOS neuronal populations expressing ER $\alpha$  in the adult hypothalamus already express ER $\alpha$  at P11. Intriguingly, however, our results show that nNOS expression in the ARH, in which ER $\alpha$  immunoreactivity is seen during the infantile period at P11, only becomes apparent during the juvenile period, at P23. The issues of whether circulating estrogens drive nNOS expression in the ARH and whether nNOS expression in ER $\alpha$ -immunoreactive cells is required for the onset of estradiol negative feedback on the HPG axis, require clarification.

Our double-immunolabeling data reveal that the most densely packed nNOS population of the hypothalamus occurs in the OV/MEPO, a brain region in which NO-producing neurons are known to play a role in regulating GnRH neuronal activity and function (Bellefontaine et



al., 2014; Clasadonte et al., 2008; d'Anglemont de Tassigny et al., 2007; Hanchate et al., 2012; Messina et al., 2016). Consistent with the critical involvement of estradiol in the control of nNOS activity in the preoptic region (d'Anglemont de Tassigny et al., 2007; d'Anglemont de Tassigny, Campagne, Steculorum, & Prevot, 2009; Parkash et al., 2010), a majority of OV/MEPO nNOS neurons are seen to express ER $\alpha$ . ER $\alpha$  in the OV/MEPO is also almost exclusively expressed in nNOS neurons, indicating the importance of this discrete neuronal population in sensing gonadal information. Neurons of the OV, which, like other circumventricular organs, lies outside the blood-brain barrier, are likely to have greatly facilitated access to circulating hormones including gonadal steroids (Langlet, Mullier, Bouret, Prevot, & Dehouck, 2013; Prager-Khoutorsky & Bourque, 2015) and are well positioned to convey this information to GnRH neurons.

The present study also shows that in addition to being expressed in the OV/MEPO and the ARH, nNOS is also abundantly expressed in other hypothalamic nuclei such as the PVH, VMH, and DMH, as well as in the LHA. Each of these nuclei and areas is known, like the ARH and more recently the MEPO, to be deeply involved in the regulation of energy homeostasis (Cone et al., 2001; Elmquist, Coppari, Balthasar, Ichinose, & Lowell, 2005; Saper, Chou, & Elmquist, 2002; Sawchenko, 1998; Schwartz, Woods, Porte, Seeley, & Baskin, 2000; Sutton, Myers, & Olson, 2016; Yu et al., 2016; Zhang et al., 2011). Consistent with the potential role of nNOS in metabolic pathways, recent reports have shown that mice lacking the receptor for the anorexigenic hormone leptin specifically in nNOS neurons display hyperphagic obesity (Leshan et al., 2012), and that introducing an nNOS-null mutation into leptin-deficient mice significantly reduces the obese phenotype of these mice (Bellefontaine et al., 2014). In particular, PVH neurons containing nNOS have been shown to be critically involved in PVH regulated energy balance (Sutton et al., 2016) since selective activation of nNOS neurons in the PVH is found to regulate both feeding and energy expenditure (Sutton et al., 2014). Interestingly, our present results show that the great majority of nNOS cells in the VMH also express the receptor for estradiol, which, in addition to its critical functions as a reproductive hormone, plays a vital role in the regulation of energy balance (Gao et al., 2007; Park et al., 2011). In contrast, nNOS/ER $\alpha$  double-labeled cells are rarely seen in the DMH or the LHA, or in the ventral premammillary nucleus, which has been shown to relay metabolic information to GnRH neurons (Donato et al., 2011), despite its abundant nNOS expression.

On the whole, our current findings on nNOS expression in adult female mice agree well with previous observations in the rat hypothalamus (Herbison et al., 1996; Yamada, Emson, & Hokfelt, 1996) and the mouse brain (Gotti, Sica, Viglietti-Panzica, & Panzica, 2005; Sica, Martini, Viglietti-Panzica, & Panzica, 2009), with some exceptions. Most differences observed between the studies involved differences in signal intensity. For example, although Gotti et al. reported weak nNOS staining in the OV, we detected heavy staining in this area, with nNOS neurons being densely packed. These apparent discrepancies may be due to sex differences, since nNOS expression in the hypothalamus has been shown to be sexually dimorphic (Knoll, Wolfe, & Tobet, 2007).

The present study also demonstrates that most nNOS neurons of the hypothalamus possess a glutamatergic phenotype, but that nNOS neurons of the ARH appear to be GABAergic.

Notably, the ARH is the only hypothalamic nucleus in which nNOS is found in a subpopulation of GABAergic interneurons expressing parvalbumin and usually found in the medial septum, the cortical areas, and the cerebellum (Ango et al., 2004; Chattopadhyaya et al., 2004). Although no study has characterized the morphology and electrophysiology of these cells population, further investigation is needed to define their specific role in the ARH circuit function. The prevalence of glutamatergic signaling in nNOS-expressing neurons of the OV/MEPO suggests that the glutamate-mediated activation of nNOS via the NMDA receptor, responsible for the  $\text{Ca}^{2+}$  influx activating the enzyme (Garthwaite et al., 1988), could occur locally through autocrine and paracrine pathways and that input from other brain regions may play only a modulatory role. While glutamatergic nNOS neurons in the OV/MEPO are intermingled with GnRH neuronal cells bodies, most of which are also glutamatergic (only a few express *Gad67*) (Dumalska et al., 2008), GABAergic nNOS neurons in the ARH appear to be morphologically associated with GnRH axon terminals.

In conclusion, this immunohistochemical study provides detailed and novel information about the spatial and temporal distribution of nNOS and  $\text{ER}\alpha$  in the female mouse hypothalamus. In addition, it reveals critical sites in which nNOS expression changes during postnatal development, and identifies distinct subsets of hypothalamic nNOS neurons according to their neurochemical phenotype (Figure 7). These data support the role of hypothalamic nNOS in the regulation of reproductive and energy homeostasis both in developing and mature animals (Chachlaki, Garthwaite, & Prevot, 2017).

## ACKNOWLEDGMENTS

This work was supported by doctoral fellowships from the University of Lille to K.C. and S.M., Inserm grant U1172, the Agence Nationale de la Recherche, ANR (grant ANR-14-CE12-0015-01 RoSes and GnRH to P.G. and F.A.), the Fondation pour la Recherche Médicale, FRM (DEQ20120323700 to V.P.), the NIH R01DK092587 (H.M.) and NIH T32DK064584 (E.Q.C.) and the ERC COST action BM1015 coordinated by Dr. Nelly Pitteloud, Lausanne (V.P., P.G. and E.H.). We thank Dr. S Rasika for editing the manuscript and Noémie Eyraud for expert technical assistance.

## REFERENCES

- Ango F, di Cristo G, Higashiyama H, Bennett V, Wu P, & Huang ZJ (2004). Ankyrin-based subcellular gradient of neurofascin, an immunoglobulin family protein, directs GABAergic innervation at purkinje axon initial segment. *Cell*, 119, 257–272. [PubMed: 15479642]
- Bakker J, De Mees C, Douhard Q, Balthazart J, Gabant P, Szpirer J, & Szpirer C (2006). Alpha-fetoprotein protects the developing female mouse brain from masculinization and defeminization by estrogens. *Nature Neuroscience*, 9, 220–226. [PubMed: 16388309]
- Bellefontaine N, Chachlaki K, Parkash J, Vanacker C, Colledge W, d'Anglemonet de Tassigny X, Prevot V (2014). Leptin-dependent neuronal NO signaling in the preoptic hypothalamus facilitates reproduction. *Journal of Clinical Investigation*, 124, 2550–2559. [PubMed: 24812663]
- Brann DW, & Mahesh VB (1991). Endogenous excitatory amino acid involvement in the preovulatory and steroid-induced surge of gonadotropins in the female rat. *Endocrinology*, 128, 1541–1547. [PubMed: 1900231]
- Brock O, De Mees C, & Bakker J (2015). Hypothalamic expression of oestrogen receptor alpha and androgen receptor is sex-, age- and region-dependent in mice. *Journal of Neuroendocrinology*, 27, 264276.
- Chachlaki K, Garthwaite G, & Prevot V (2017). The gentle art of saying NO: How nitric oxide gets things done in the preoptic region of the brain. *Nature Reviews Endocrinology*. 10.1038/nrendo.2017.69

- Chattopadhyaya B, Di Cristo G, Higashiyama H, Knott GW, Kuhlman SJ, Welker E, & Huang ZJ (2004). Experience and activity-dependent maturation of perisomatic GABAergic innervation in primary visual cortex during a postnatal critical period. *Journal of Neuroscience*, 24, 9598–9611. [PubMed: 15509747]
- Cheong RY, Czielesky K, Porteous R, & Herbison AE (2015). Expression of ESR1 in glutamatergic and GABAergic neurons is essential for normal puberty onset, estrogen feedback, and fertility in female mice. *Journal of Neuroscience*, 35, 14533–14543. [PubMed: 26511244]
- Clasadonte J, Poulain P, Beauvillain JC, & Prevot V (2008). Activation of neuronal nitric oxide release inhibits spontaneous firing in adult gonadotropin-releasing hormone neurons: A possible local synchronizing signal. *Endocrinology*, 149, 587–596. [PubMed: 18006627]
- Claypool LE, Kasuya E, Saitoh Y, Marzban F, & Terasawa E (2000). N-methyl D,L-aspartate induces the release of luteinizing hormone-releasing hormone in the prepubertal and pubertal female rhesus monkey as measured by in vivo push-pull perfusion in the stalk-median eminence. *Endocrinology*, 141, 219–228. [PubMed: 10614642]
- Cone RD, Cowley MA, Butler AA, Fan W, Marks DL, & Low MJ (2001). The arcuate nucleus as a conduit for diverse signals relevant to energy homeostasis. *International Journal of Obesity and Related Metabolic Disorders*, 25 Suppl 5, S63–67.
- Crespo C, Gracia-Llanes FJ, Blasco-Ibanez JM, Gutierrez-Mecinas M, Marques-Mari AI, & Martinez-Guijarro FJ (2003). Nitric oxide synthase containing periglomerular cells are GABAergic in the rat olfactory bulb. *Neuroscience Letters*, 349, 151–154. [PubMed: 12951191]
- d'Anglemont de Tassigny X, Campagne C, Dehouck B, Leroy D, Holstein GR, Beauvillain JC, ... Prevot V (2007). Coupling of neuronal nitric oxide synthase to NMDA receptors via postsynaptic density-95 depends on estrogen and contributes to the central control of adult female reproduction. *Journal of Neuroscience*, 27, 61036114.
- d'Anglemont de Tassigny X, Campagne C, Steculorum S, & Prevot V (2009). Estradiol induces physical association of neuronal nitric oxide synthase with NMDA receptor and promotes nitric oxide formation via estrogen receptor activation in primary neuronal cultures. *Journal of Neurochemistry*, 109, 214–224.
- Donato J, Jr., Cravo RM, Frazao R, Gautron L, Scott MM, Lachey J, ... Elias CF (2011). Leptin's effect on puberty in mice is relayed by the ventral premammillary nucleus and does not require signaling in Kiss1 neurons. *Journal of Clinical Investigation*, 121, 355–368. [PubMed: 21183787]
- Dumalska I, Wu M, Morozova E, Liu R, van den Pol A, & Alreja M (2008). Excitatory effects of the puberty-initiating peptide kisspeptin and group I metabotropic glutamate receptor agonists differentiate two distinct subpopulations of gonadotropin-releasing hormone neurons. *Journal of Neuroscience*, 28, 8003–8013. [PubMed: 18685025]
- Edelmann M, Wolfe C, Scordalakes EM, Rissman EF, & Tobet S (2007). Neuronal nitric oxide synthase and calbindin delineate sex differences in the developing hypothalamus and preoptic area. *Developmental Neurobiology*, 67, 1371–1381. [PubMed: 17638388]
- Elmquist JK, Coppari R, Balthasar N, Ichinose M, & Lowell BB (2005). Identifying hypothalamic pathways controlling food intake, body weight, and glucose homeostasis. *Journal of Comparative Neurology*, 493, 63–71. [PubMed: 16254991]
- Friend KE, Resnick EM, Ang LW, & Shupnik MA (1997). Specific modulation of estrogen receptor mRNA isoforms in rat pituitary throughout the estrous cycle and in response to steroid hormones. *Molecular and Cellular Endocrinology*, 131, 147–155. [PubMed: 9296373]
- Fujimoto H, Konno K, Watanabe M, & Jinno S (2016). Late postnatal shifts of parvalbumin and nitric oxide synthase expression within the GABAergic and glutamatergic phenotypes of inferior colliculus neurons. *Journal of Comparative Neurology*, 525, 868–884. [PubMed: 27560447]
- Gao Q, Mezei G, Nie Y, Rao Y, Choi CS, Bechmann I, ... Horvath TL (2007). Anorectic estrogen mimics leptin's effect on the rewiring of melanocortin cells and Stat3 signaling in obese animals. *Nature Medicine*, 13, 89–94.
- Garthwaite J (2008). Concepts of neural nitric oxide-mediated transmission. *European Journal of Neuroscience*, 27, 2783–2802. [PubMed: 18588525]
- Garthwaite J (2016). From synaptically localized to volume transmission by nitric oxide. *Journal of Physiology*, 594, 9–18. [PubMed: 26486504]

- Garthwaite J, Charles SL, & Chess-Williams R (1988). Endothelium-derived relaxing factor release on activation of NMDA receptors suggests role as intercellular messenger in the brain. *Nature*, 336, 385-388.
- Germain BJ, Campbell PS, & Anderson JN (1978). Role of the serum estrogen-binding protein in the control of tissue estradiol levels during postnatal development of the female rat. *Endocrinology*, 103, 1401–1410. [PubMed: 84755]
- Giuli G, Luzzi A, Poyard M, & Guellaen G (1994). Expression of mouse brain soluble guanylyl cyclase and NO synthase during ontogeny. *Brain Research. Developmental Brain Research*, 81, 269–283. [PubMed: 7529143]
- Gotti S, Sica M, Viglietti-Panzica C, & Panzica G (2005). Distribution of nitric oxide synthase immunoreactivity in the mouse brain. *Microscopy Research and Technique*, 68, 13–35. [PubMed: 16208717]
- Gyurko R, Leupen S, & Huang PL (2002). Deletion of exon 6 of the neuronal nitric oxide synthase gene in mice results in hypogonadism and infertility. *Endocrinology*, 143, 2767–2774. [PubMed: 12072412]
- Hanchate NK, Parkash J, Bellefontaine N, Mazur D, Colledge WH, d'Anglemont de Tassigny X, & Prevot V (2012). Kisspeptin-GPR54 signaling in mouse NO-synthesizing neurons participates in the hypothalamic control of ovulation. *Journal of Neuroscience*, 32, 932–945. [PubMed: 22262891]
- Herbison AE (2016). Control of puberty onset and fertility by gonadotropin-releasing hormone neurons. *Nature Reviews Endocrinology*, 12, 452–466.
- Herbison AE, Simonian SX, Norris PJ, & Emson PC (1996). Relationship of neuronal nitric oxide synthase immunoreactivity to GnRH neurons in the ovariectomized and intact female rat. *Journal of Neuroendocrinology*, 8, 73–82. [PubMed: 8932739]
- Hrabovszky E, Molnar CS, Sipos MT, Vida B, Ciofi P, Borsay BA, ... Liposits Z (2011). Sexual dimorphism of kisspeptin and neurokinin B immunoreactive neurons in the infundibular nucleus of aged men and women. *Frontiers in Endocrinology (Lausanne)*, 2, 80.
- Hrabovszky E, Turi GF, Kallo I, & Liposits Z (2004). Expression of vesicular glutamate transporter-2 in gonadotropin-releasing hormone neurons of the adult male rat. *Endocrinology*, 145, 4018–4021. [PubMed: 15205380]
- Huang PL, Dawson TM, Brecht DS, Snyder SH, & Fishman MC (1993). Targeted disruption of the neuronal nitric oxide synthase gene. *Cell*, 75, 1273–1286. [PubMed: 7505721]
- Jarvie BC, & Hentges ST (2012). Expression of GABAergic and glutamatergic phenotypic markers in hypothalamic proopiomelanocortin neurons. *Journal of Comparative Neurology*, 520, 3863–3876. [PubMed: 22522889]
- Knoll JG, Wolfe CA, & Tobet SA (2007). Estrogen modulates neuronal movements within the developing preoptic area-anterior hypothalamus. *European Journal of Neuroscience*, 26, 1091–1099. [PubMed: 17767488]
- Langlet F, Mullier A, Bouret SG, Prevot V, & Dehouck B (2013). Tanycyte-like cells form a blood-cerebrospinal fluid barrier in the circumventricular organs of the mouse brain. *Journal of Comparative Neurology*, 521, 3389–3405. [PubMed: 23649873]
- Lein ES, Hawrylycz MJ, Ao N, Ayres M, Bensinger A, Bernard A, ... Jones AR (2007). Genome-wide atlas of gene expression in the adult mouse brain. *Nature*, 445, 168–176. [PubMed: 17151600]
- Leshan RL, Greenwald-Yarnell M, Patterson CM, Gonzalez IE, & Myers MG, Jr. (2012). Leptin action through hypothalamic nitric oxide synthase-1-expressing neurons controls energy balance. *Nature Medicine*, 18, 820–823.
- Lin LH (2009). Glutamatergic neurons say NO in the nucleus tractus solitarius. *Journal of Chemical Neuroanatomy*, 38, 154–165. [PubMed: 19778681]
- Marshall CJ, Desrozier E, McLennan T, & Campbell RE (2016). Defining subpopulations of arcuate nucleus GABA neurons in male, female and prenatally androgenized female mice. *Neuroendocrinology* 10.1159/000452105
- Martin C, Navarro VM, Simavli S, Vong L, Carroll RS, Lowell BA, & Kaiser UB (2014). Leptin-responsive GABAergic neurons regulate fertility through pathways that result in reduced kisspeptinergic tone. *Journal of Neuroscience*, 34, 6047–6056. [PubMed: 24760864]

- Messina A, Langlet F, Chachlaki K, Roa J, Rasika S, Jouy N, ... Prevot V (2016). A microRNA switch regulates the rise in hypothalamic GnRH production before puberty. *Nature Neuroscience*, 19, 835–844. [PubMed: 27135215]
- Oakley AE, Clifton DK, & Steiner RA (2009). Kisspeptin signaling in the brain. *Endocrine Reviews*, 30, 713–743. [PubMed: 19770291]
- Okamura H, Yokosuka M, & Hayashi S (1994). Estrogenic induction of NADPH-diaphorase activity in the preoptic neurons containing estrogen receptor immunoreactivity in the female rat. *Journal of Neuroendocrinology*, 6, 597–601. [PubMed: 7894461]
- Park CJ, Zhao Z, Glidewell-Kenney C, Lazic M, Chambon P, Krust A, ... Levine JE (2011). Genetic rescue of nonclassical ERalpha signaling normalizes energy balance in obese Eralpha-null mutant mice. *Journal of Clinical Investigation*, 121, 604–612. [PubMed: 21245576]
- Parkash J, d'Anglemon de Tassigny X, Bellefontaine N, Campagne C, Mazure D, Buee-Scherrer V, & Prevot V (2010). Phosphorylation of N-methyl-D-aspartic acid receptor-associated neuronal nitric oxide synthase depends on estrogens and modulates hypothalamic nitric oxide production during the ovarian cycle. *Endocrinology*, 151, 2723–2735. [PubMed: 20371700]
- Pinilla L, Aguilar E, Dieguez C, Millar RP, & Tena-Sempere M (2012). Kisspeptins and reproduction: physiological roles and regulatory mechanisms. *Physiological Reviews*, 92, 1235–1316. [PubMed: 22811428]
- Prager-Khoutorsky M, & Bourque CW (2015). Anatomical organization of the rat organum vasculosum laminae terminalis. *American Journal of Physiology. Regulatory, Integrative and Comparative Physiology*, 309, R324–337. [PubMed: 26017494]
- Prevot V (2015). Puberty in mice and rats In Plant TM, & Zeleznik J (Eds.) *Knobil and Neill's physiology of reproduction* (pp. 1395–1439). New York: Elsevier.
- Risold PY, & Swanson LW (1997). Connections of the rat lateral septal complex. *Brain Research. Brain Research Reviews*, 24, 115–195. [PubMed: 9385454]
- Saper CB, Chou TC, & Elmquist JK (2002). The need to feed: homeostatic and hedonic control of eating. *Neuron*, 36, 199–211. [PubMed: 12383777]
- Sawchenko PE (1998). Toward a new neurobiology of energy balance, appetite, and obesity: The anatomists weigh in. *Journal of Comparative Neurology*, 402, 435–441. [PubMed: 9862319]
- Schwartz MW, Woods SC, Porte D, Jr., Seeley RJ, & Baskin DG (2000). Central nervous system control of food intake. *Nature*, 404, 661–671. [PubMed: 10766253]
- Sica M, Martini M, Viglietti-Panzica C, & Panzica G (2009). Estrous cycle influences the expression of neuronal nitric oxide synthase in the hypothalamus and limbic system of female mice. *BMC Neuroscience*, 10, 78. [PubMed: 19604366]
- Steinert JR, Chernova T, & Forsythe ID (2010). Nitric oxide signaling in brain function, dysfunction, and dementia. *Neuroscientist*, 16, 435–452. [PubMed: 20817920]
- Sutton AK, Myers MG, Jr., & Olson DP (2016). The role of PVH circuits in leptin action and energy balance. *Annual Review of Physiology*, 78, 207–221.
- Sutton AK, Pei H, Burnett KH, Myers MG, Jr., Rhodes CJ, & Olson DP (2014). Control of food intake and energy expenditure by Nos1 neurons of the paraventricular hypothalamus. *Journal of Neuroscience*, 34, 15306–15318. [PubMed: 25392498]
- Swanson LW, & Cowan WM (1979). The connections of the septal region in the rat. *Journal of Comparative Neurology*, 186, 621–655. [PubMed: 15116692]
- Tricoire L, & Vitalis T (2012). Neuronal nitric oxide synthase expressing neurons: A journey from birth to neuronal circuits. *Frontiers in Neural Circuits*, 6, 82. [PubMed: 23227003]
- Urbanski HF, & Ojeda SR (1990). A role for N-methyl-D-aspartate (NMDA) receptors in the control of LH secretion and initiation of female puberty. *Endocrinology*, 126, 1774–1776. [PubMed: 1968384]
- von Bartheld CS, & Schober A (1997). Nitric oxide synthase in learning-relevant nuclei of the chick brain: morphology, distribution, and relation to transmitter phenotypes. *Journal of Comparative Neurology*, 383, 135–152. [PubMed: 9182844]
- Vong L, Ye C, Yang Z, Choi B, Chua S, Jr., & Lowell BB (2011). Leptin action on GABAergic neurons prevents obesity and reduces inhibitory tone to POMC neurons. *Neuron*, 71, 142–154. [PubMed: 21745644]

- Yamada K, Emson P, & Hokfelt T (1996). Immunohistochemical mapping of nitric oxide synthase in the rat hypothalamus and colocalization with neuropeptides. *Journal of Chemical Neuroanatomy*, 10, 295–316. [PubMed: 8811420]
- Yu S, Qualls-Creekmore E, Rezai-Zadeh K, Jiang Y, Berthoud HR, Morrison CD, ... Munzberg H (2016). Glutamatergic preoptic area neurons that express leptin receptors drive temperature-dependent body weight homeostasis. *Journal of Neuroscience*, 36, 5034–5046. [PubMed: 27147656]
- Zhang Y, Kerman IA, Laque A, Nguyen P, Faouzi M, Louis GW, ... Munzberg H (2011). Leptin-receptor-expressing neurons in the dorsomedial hypothalamus and median preoptic area regulate sympathetic brown adipose tissue circuits. *Journal of Neuroscience*, 31, 1873–1884. [PubMed: 21289197]
- Zuure WA, Roberts AL, Quennell JH, & Anderson GM (2013). Leptin signaling in GABA neurons, but not glutamate neurons, is required for reproductive function. *Journal of Neuroscience*, 33, 17874–17883. [PubMed: 24198376]



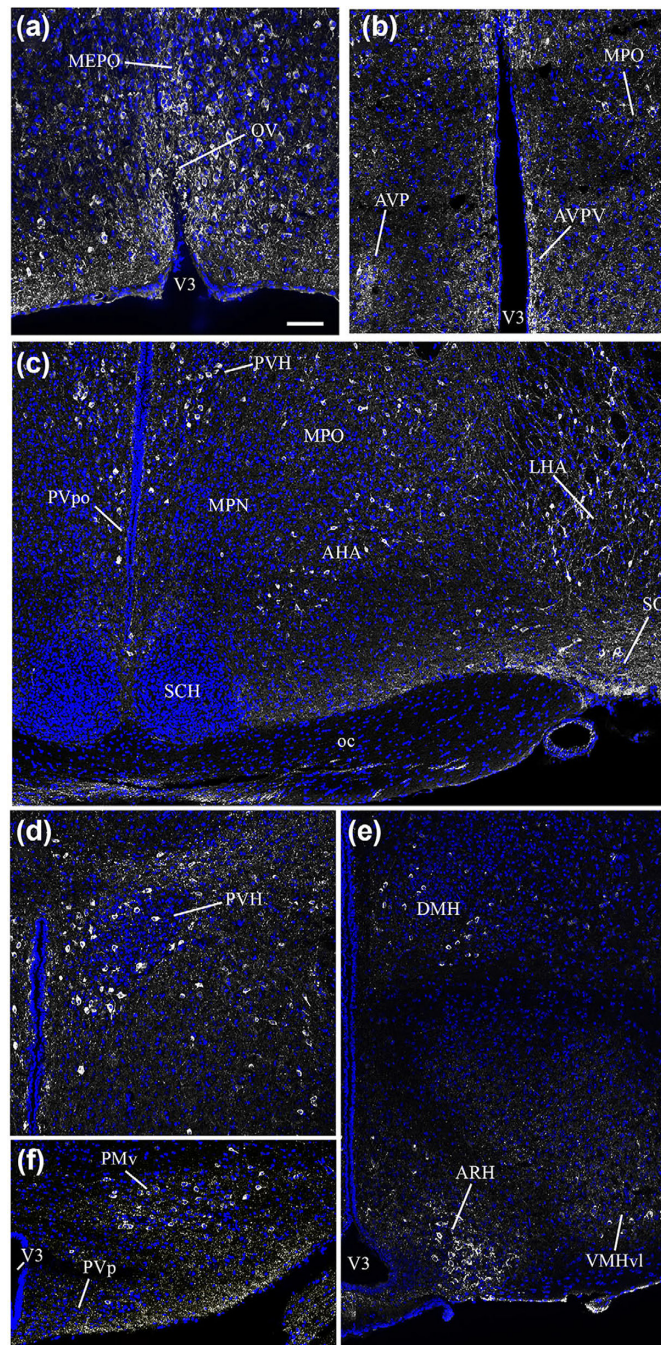


**FIGURE 1.**

Photomicrographs showing the distribution of nNOS immunoreactivity in distinct hypothalamic nuclei as seen in coronal sections of the adult female mouse brain. nNOS immunoreactivity (white labeling) is readily visualized in neurons of the preoptic area; labeling is evident in the regions of the organum vasculosum laminae terminalis (OV, a), median preoptic nucleus (MEPO, a), anteroventral preoptic nucleus (AVP, b), anteroventral periventricular nucleus (AVPV, b), and medial preoptic region (MPO, b). nNOS immunoreactivity was also detected in the anterior hypothalamic nucleus (AHN, c), lateral

hypothalamic area (LHA, c) and supraoptic nucleus (SO, c), with rare neurons also present in the periventricular nucleus of the hypothalamus (PVp, f). nNOS-expressing neurons were also visualized in the paraventricular nucleus of the hypothalamus (PVH, d), the dorsomedial nucleus of the hypothalamus (DMH, e), the ventrolateral part of the ventromedial nucleus of the hypothalamus (VMH, e), the arcuate nucleus of the hypothalamus (ARH, e) and the ventral premammillary nucleus (PMv, f). Sections are counterstained using Hoechst (blue) to visualize cell nuclei and identify the morphological limits of each hypothalamic structure. 3V: third ventricle. Scale bar =100  $\mu\text{m}$  in (a), (b), (d) and (f), and 200  $\mu\text{m}$  in (c) and (e)



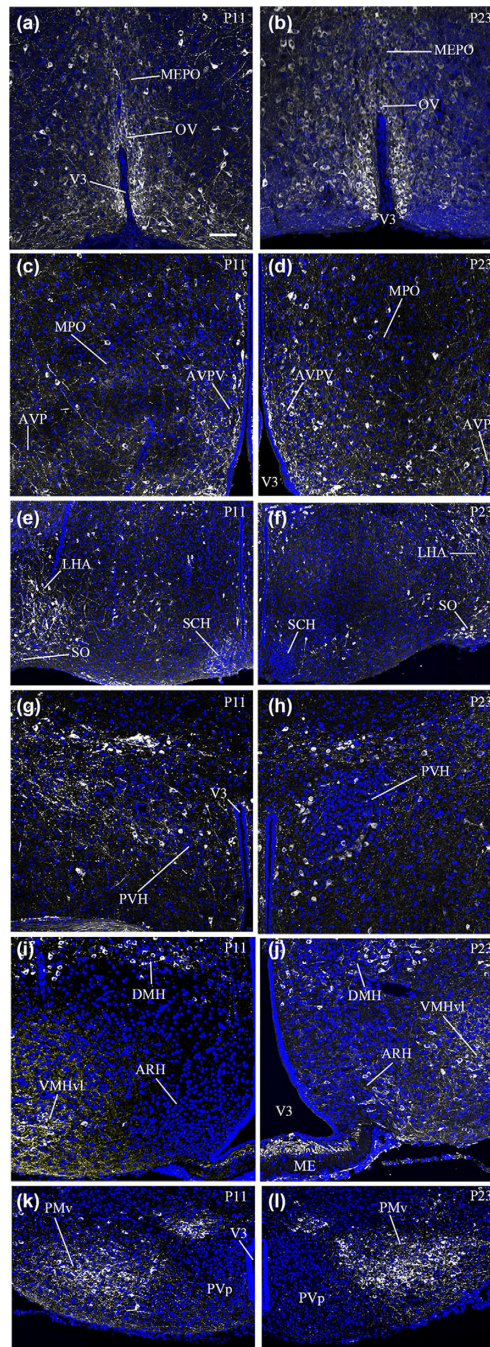
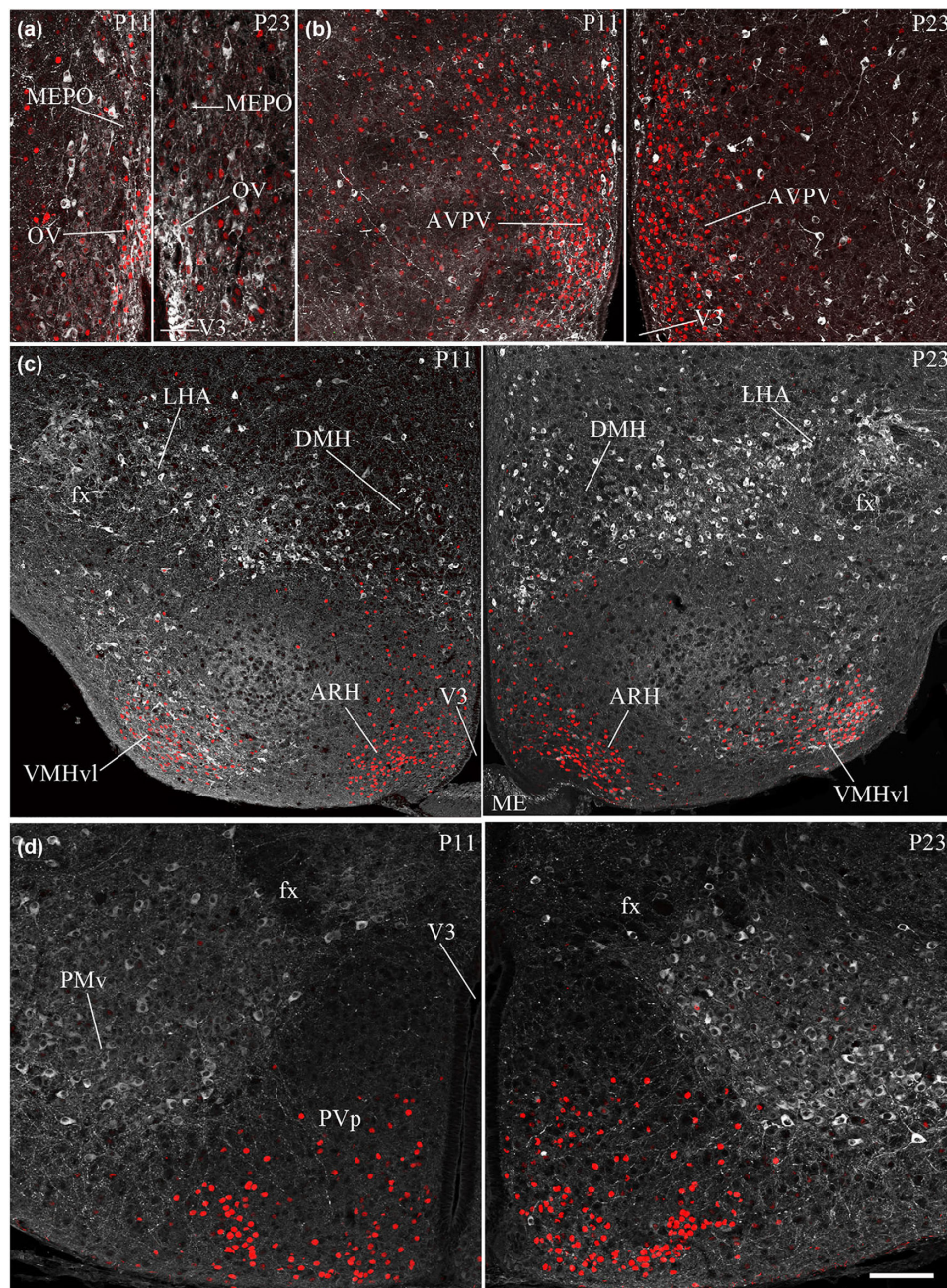


**FIGURE 2.**

Representative photomicrographs demonstrating the expression of nNOS immunoreactivity in the infantile and juvenile hypothalamus. Note the absence of nNOS immunoreactivity (white labeling) in the arcuate nucleus of the hypothalamus (ARH) in infantile mice (P11; i) and its appearance in the ARH of juvenile mice (P23; j). In contrast, nNOS immunoreactivity is present in the suprachiasmatic nucleus (SCH) in infantile mice (e), while it is mostly absent during the juvenile period (f). OV, organum vasculosum laminae terminalis (a, b); MEPO, median preoptic nucleus (a, b); AVP, anteroventral preoptic nucleus

(c, d); AVPV, anteroventral periventricular nucleus of the hypothalamus (c, d); MPO, medial preoptic area (c, d); PVH, paraventricular nucleus of the hypothalamus (g, h); DMH, dorsomedial nucleus of the hypothalamus (i, j); VMHvl, ventrolateral part of the ventromedial nucleus of the hypothalamus (i, j); PMv, ventral premammillary nucleus (k, l). Sections are counterstained using Hoechst (blue) to visualize cell nuclei and identify the morphological limits of each hypothalamic structure. 3V: third ventricle. Scale bar =100  $\mu$ m in (a-d), (g) and (h), 150  $\mu$ m in (k), (l) and 200  $\mu$ m in (e), (f), (i) and (j)

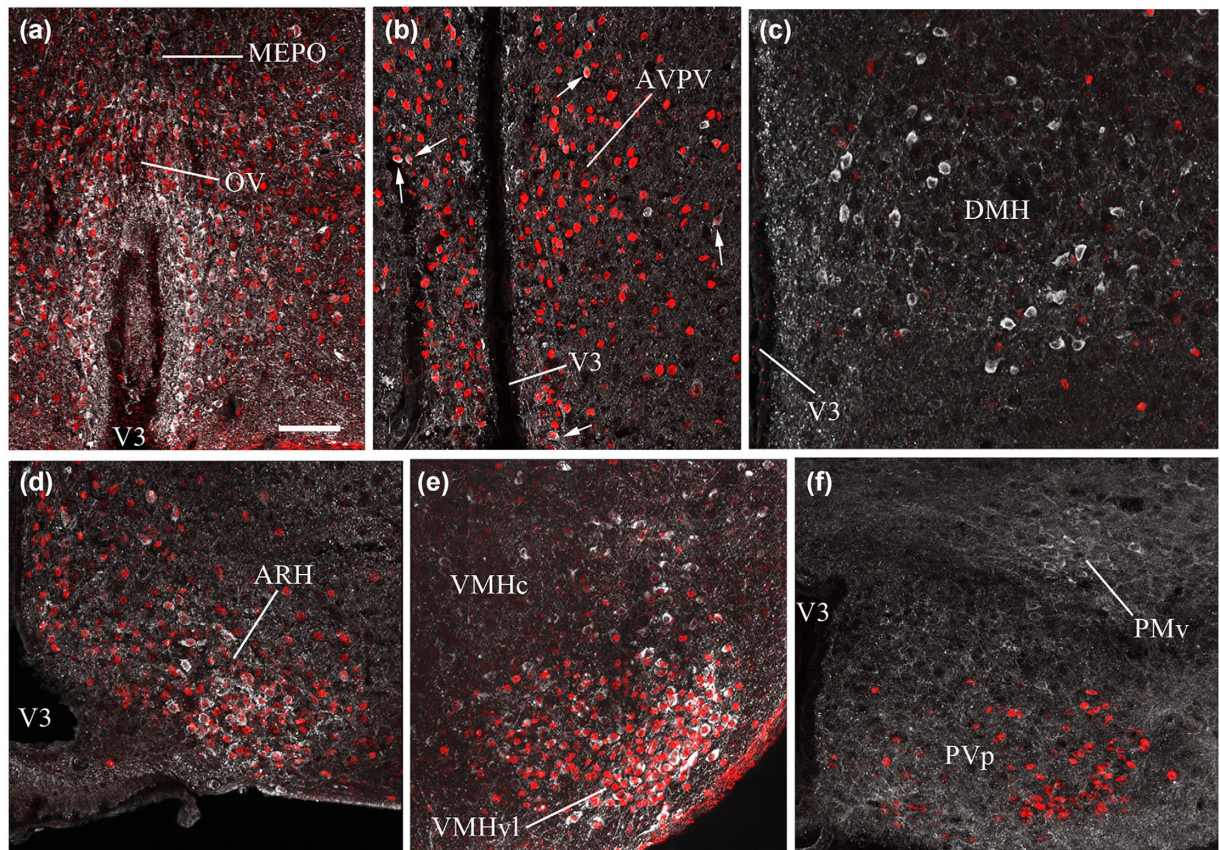




**FIGURE 3.**

Representative images showing estrogen receptor alpha (ERα)- and nNOS-immunolabeling in the hypothalamus of P11 infantile and P23 juvenile mice. nNOS (white labeling) and ERα (red nuclear labeling) are highly colocalized in the organum vasculosum laminae terminalis (OV), median preoptic nucleus (MEPO) (a), anteroventral periventricular nucleus of the hypothalamus (AVPV, b), and the ventromedial hypothalamic nucleus (VMH) in the tuberal hypothalamus (c), in both infantile and juvenile mice, as well as in the arcuate nucleus of the hypothalamus (ARH) in juvenile mice (c). Scale bar = 100 μm in (a) and (d), 150 μm in (b) and 200 μm in (c)

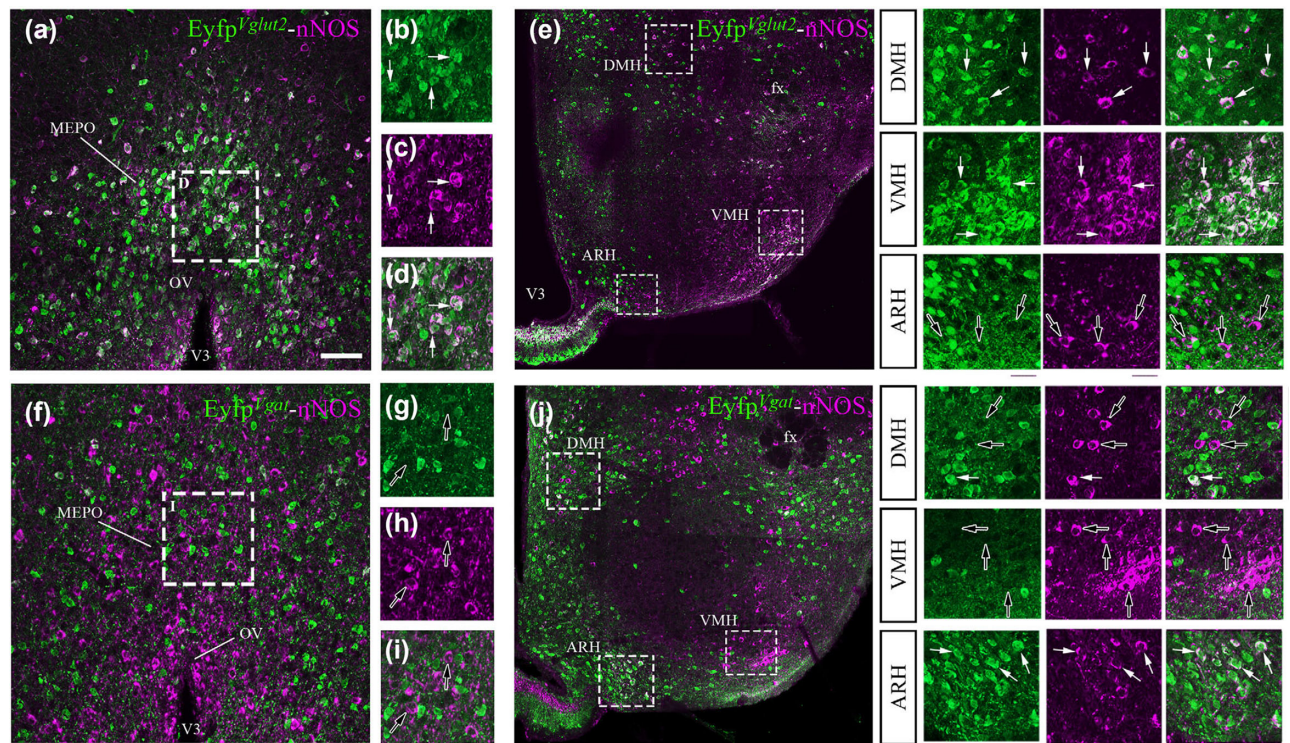




**FIGURE 4.**

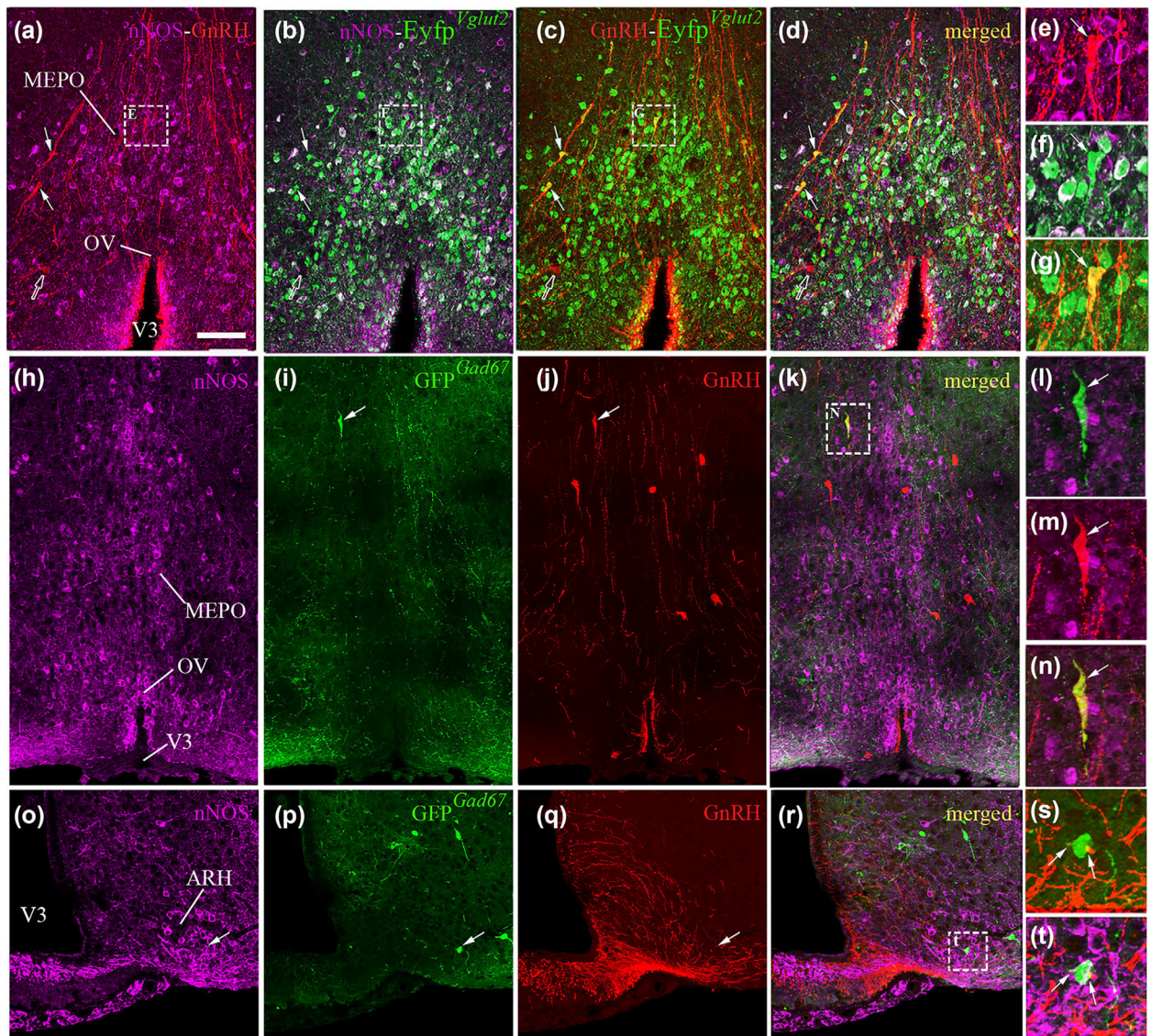
Representative images showing estrogen receptor alpha (ERα)- and nNOS-immunolabeling in the hypothalamus of adult mice. Similarly to what was observed in juvenile mice (P23), nNOS (white labeling) and ERα (red nuclear labeling) are highly colocalized in the organum vasculosum laminae terminalis (OV), median preoptic nucleus (MEPO) (a), anteroventral periventricular nucleus of the hypothalamus (white arrows) (AVPV, b), arcuate nucleus of the hypothalamus (ARH; d) and ventromedial hypothalamic nucleus (VMH; e). In contrast, colocalization is not evident in the dorsomedial hypothalamic nucleus (DMH; c), the periventricular hypothalamic nucleus (PVp; f) or the ventral premammillary nucleus (PMv; f). Scale bar = 100 μm



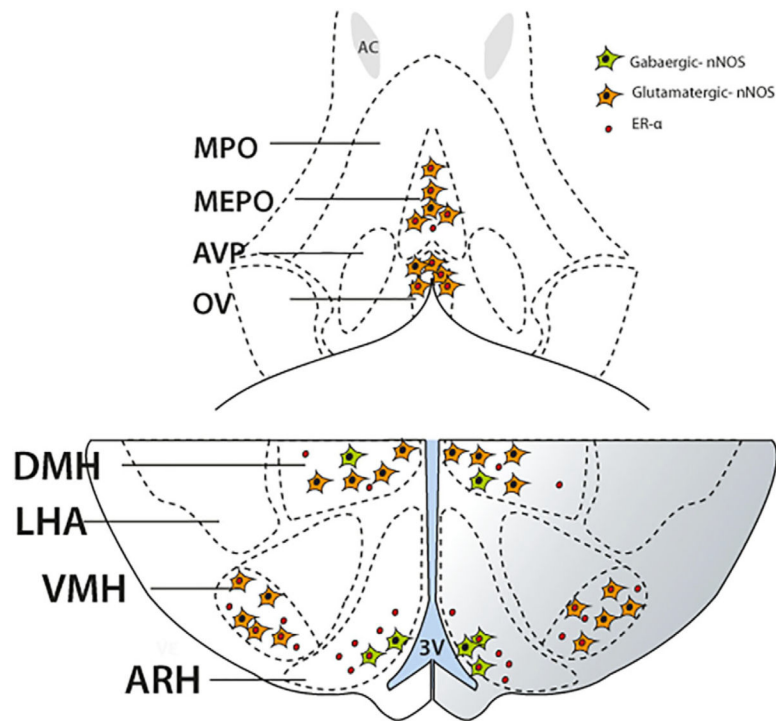
**FIGURE 5.**

Representative images of nNOS immunoreactivity in adult female EYFP<sup>Vglut2</sup> and EYFP<sup>Vgat</sup> mice. nNOS-immunoreactive neurons (purple labeling) of the preoptic region (a), the dorsomedial nucleus of the hypothalamus (DMH; e, upper inset) and the ventromedial nucleus of the hypothalamus (VMH; e, middle inset) are immunoreactive for enhanced yellow fluorescent protein (YFP-IR, green) in EYFP<sup>Vglut2</sup> mice but not in EYFP<sup>Vgat</sup> mice (f, j). In contrast, nNOS neurons of the arcuate nucleus of the hypothalamus (ARH) show YFP-IR in EYFP<sup>Vgat</sup> mice (j) but not in EYFP<sup>Vglut2</sup> mice (e, lower inset). White arrowheads indicate nNOS and YFP colocalization; empty arrowheads show nNOS single-labeled cells. Scale bar = 100 μm (50 μm in insets)



**FIGURE 6.**

Representative images showing nNOS and GnRH immunoreactive neurons in EYFP<sup>Vgut2</sup> and GFP<sup>Gad67</sup> female mice. Colocalization of the enhanced yellow fluorescent protein (YFP-IR, green) is evident in both nNOS-immunoreactive cells (purple; b, f) and GnRH-immunoreactive neurons (red; c, g) in the preoptic region of adult female EYFP<sup>Vgut2</sup> mice (a-g). Expression of green fluorescent protein (GFP) driven by the *Gad67* promoter is absent in nNOS-immunoreactive cells (purple) of the preoptic region (h-i), while it is occasionally expressed in GnRH-immunoreactive neurons (red; i-n). In the arcuate nucleus of the adult female hypothalamus (ARH), nNOS-immunoreactive neurons expressing GFP<sup>Gad67</sup> (o-p, t) are surrounded by GnRH-immunoreactive fibers (red; q, s, t). Scale bar = 100 μm (25 μm in insets)

**FIGURE 7.**

Schematic diagram demonstrating the distribution and phenotype of nNOS immunoreactive neurons in the preoptic (upper panel) and the tuberal (bottom panel) regions of the hypothalamus of adult female mice. The majority of the nNOS-immunoreactive cells of the organum vasculosum laminae terminalis (OV) and the median preoptic nucleus (MEPO) are of a glutama-tergic phenotype (orange), and a substantial proportion of them also express the estrogen receptor  $\alpha$  (ER $\alpha$ ; red dot). In the tuberal region of the hypothalamus, nNOS-immunoreactive neurons are divided into distinct subpopulations depending on the main neurotransmitter they express, with or without expression of the estrogen receptor. More specifically, in the region of the arcuate nucleus (ARH), nNOS neurons are mostly members of the GABAergic population of cells (green), and a high proportion of them express ER $\alpha$ . In the ventromedial nucleus of the hypothalamus (VMH), nNOS neurons are glutamatergic and most of them express ER $\alpha$  immunoreactivity. The dorsomedial nucleus of the hypothalamus (DMH) contains both GABAergic and glutamatergic nNOS-immunoreactive neurons, with glutamatergic nNOS neurons being the predominant population. Only rare nNOS neurons in the DMH were seen to express ER $\alpha$ .

**Table 1**

Primary antibodies used in this study

Antibody	Animal	Antigen	Manufacturer and cat. no	Characterization
GFP	Chicken, polyclonal	Recombinant full length GFP	Abcam Ab 13970	Jarvie and Hentges (2012)
nNOS	Sheep, polyclonal	Full length Rat NOS1 protein	Generous gift from Dr. P. C. Emson	Herbison et al. (1996)
ERα	Rabbit, polyclonal	TYYPPEAEGFPNTI corresponding to the C-terminus of mouse/rat Estrogen receptor alpha	Millipore 06-935	Friend, Resnick, Ang, and Shupnik (1997)
GnRH	Guinea-pig, polyclonal	Mammalian GnRH	EH#1018 from Dr. E. Hrabovszky	Hrabovszky et al. (2011)

**Table 2**

Relative densities of nNOS immunoreactivity in the postnatal and adult brain

	<b>P11</b>	<b>P23</b>	<b>Adult</b>	
LPO: lateral preoptic area	++(+)	++(+)	++(+)	Level 49–50
MPO: medial preoptic area		++	++	
OV: organum vasculosum laminae terminalis	++++	++++	++++	
MEPO: median preoptic nucleus	+++	+++	+++	
AVPV: anteroventral periventricular nucleus hypothalamus	+	+	+	Level 53–54
AVP: anteroventral preoptic nucleus	++	++	++	
MPN: medial preoptic nucleus				
lateral part	+(+)	+(+)	+(+)	
medial part	(+)	(+)	(+)	
AHN: anterior hypothalamic nucleus				Level 58–61
central part	++	(+)	(+)	
anterior part	++	++	+	
LHA: lateral hypothalamic area	++	++	+	
SCH: suprachiasmatic hypothalamic nucleus	+	+/-	-(+)	
SON: supraoptic nucleus	+(+)	++	++(+)	
PVHap: paraventricular nucleus, anterior parvicellular part	++	++	++	
Pva: periventricular hypothalamic nucleus, anterior part	+	+	+	
PVpo: preoptic periventricular nucleus	++	++	+(+)	
ARH: arcuate nucleus	-	+	+	Level 70–72
VMH: ventromedial hypothalamic nucleus				
dorsomedial part	+/-	+/-	+/-	
central part	-	-	-	
ventromedial part	++	++	++	
DMH: dorsomedial hypothalamic nucleus				
anterior part	++(+)	++(+)	++(+)	
posterior part	++	++	++	
PVp: periventricular hypothalamic nucleus, posterior part	(+)	(+)	(+)	Level 77–78
PMv: premammillary nucleus, ventral	++	++	++	
PMd: premammillary nucleus, dorsal	+(+)	+(+)	++	
PH: posterior hypothalamic nucleus	++	++	+(+)	